

## Gravitational Wave from Graviton Bremsstrahlung during Reheating

---

Yong Xu<sup>a,\*</sup>

<sup>a</sup>PRISMA<sup>+</sup> Cluster of Excellence and Mainz Institute for Theoretical Physics  
Johannes Gutenberg University, 55099 Mainz, Germany

E-mail: [yonxu@uni-mainz.de](mailto:yonxu@uni-mainz.de)

In this talk, we explore the stochastic Gravitational Waves (GW) resulting from graviton Bremsstrahlung during inflationary reheating. I start by discussing the motivation behind the study and introduce the computational formalism, with a specific emphasis on the graviton production rate. Then, I present the GW spectrum for inflaton oscillations around a quadratic potential  $\sim \phi^2$ . By generalizing the potential to  $\sim \phi^n$  with  $n > 2$ , I show that distinct features in the GW spectrum emerge depending on both the value of  $n$  and type of inflaton-matter couplings. Finally, I demonstrate that Bremsstrahlung-induced GW can serve as a novel pathway for probing the dynamics of inflationary reheating.

*Corfu Summer Institute 2023 "Workshop on Theoretical Particle Cosmology in the Early and Late Universe" (CORFU2023)*  
30 April - 6 May, 2023  
Corfu, Greece

---

\*Speaker

## 1. Introduction

Cosmic inflation stands as an elegant paradigm for addressing cosmological issues such as the horizon, flatness, and monopole problems. The simplest theory involves scalar field(s) slowly rolling down from a flat potential, driving exponential expansion of the Universe [1]. Subsequent to inflation, the energy of the inflaton must transition to other lighter degrees of freedom, interacting and ultimately forming into a thermal bath. This energy transfer can proceed through inflaton decay via trilinear couplings [2]. Due to the inherent coupling between the background metric and the energy-momentum tensor, gravitons can be generated in a radiative Bremsstrahlung process accompanying inflaton decay [3, 4]. After production these gravitons propagate throughout the universe, giving rise to a homogeneous and isotropic stochastic gravitational wave (GW) background.

In this talk, I revisit the GW spectrum generated from graviton Bremsstrahlung during inflationary reheating, which has been recently investigated Refs. [5, 6]. Here, I present a concise summary of the main findings discussed in these references. I will start by introducing the two-body inflaton decay for reheating and the three-body decay for graviton production in Section 2. The GW spectrum for an inflaton oscillating in a quadratic potential is presented in Section 3. In Section 4, I extend the analysis to potentials  $\sim \phi^n$ , discussing the novel features in the GW spectrum. I conclude with a summary in Section 5.

## 2. The Setup

In this section, I will briefly discuss the inflaton two-body decay for reheating. Following that, I will shift the focus to graviton production through a three-body decay process. Regarding reheating, we consider the scenario where the inflaton decays into a pair of lighter boson (e.g. Higgs field in the standard model) or vector-like fermion (e.g. right-handed neutrino) through the following trilinear couplings:

$$\mathcal{L}_{\text{int}} \supset -\mu \phi |\varphi|^2 - y_\psi \bar{\psi} \psi \phi, \quad (1)$$

with which the decay rates read [5]

$$\Gamma^{1 \rightarrow 2} \simeq \begin{cases} \frac{m_\phi}{8\pi} \left( \frac{\mu}{m_\phi} \right)^2 & \text{bosonic decay,} \\ \frac{m_\phi}{8\pi} y_\psi^2 & \text{fermionic decay.} \end{cases} \quad (2)$$

Here,  $m_\phi$  denotes the inflaton mass, while the couplings  $\mu$  (with mass dimension one) and  $y_\psi$  parameterize the corresponding interaction strengths. With the couplings and inflaton mass, one can estimate the reheating temperature:  $T_{\text{th}} \propto \sqrt{M_P \Gamma^{1 \rightarrow 2}}$ , where  $M_P$  denotes the reduced Planck mass.

Utilizing the expansion of the metric  $g_{\mu\nu}$  around Minkowski spacetime:  $g_{\mu\nu} \simeq \eta_{\mu\nu} + \frac{2}{M_P} h_{\mu\nu}$ , one finds gravitational interactions [7]:

$$\sqrt{-g} \mathcal{L}_{\text{int}} \supset -\frac{1}{M_P} h_{\mu\nu} T^{\mu\nu}. \quad (3)$$

Here,  $h_{\mu\nu}$  denotes the graviton field, representing a quantum fluctuation over a flat background, while  $T_{\mu\nu}$  represents the energy-momentum tensor encompassing all matter particles involved in the theory.

The interactions outlined in Eq. (3) lead to 3-body decays of the inflaton into pairs of  $\varphi$  and  $\psi$  in the final state, accompanied by the emission of a massless graviton, as depicted in Fig. 1. Applying

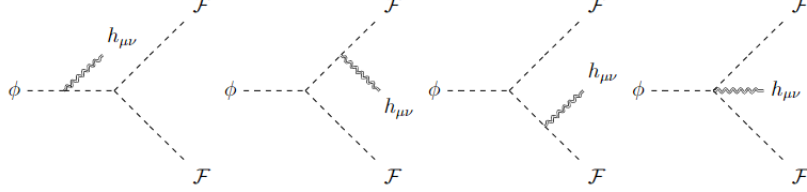


**Figure 1:** Inflaton decays into a pair of particles  $\mathcal{F} \in \{\varphi, \psi\}$  and a graviton  $h_{\mu\nu}$ .

the standard Feynman rules for the diagrams shown in Fig. 1, one can show that the differential graviton production rates are [5]

$$\frac{d\Gamma^{1\rightarrow 3}}{dE_\omega} \simeq \begin{cases} \frac{1}{128\pi^3} \left(\frac{\mu}{M_P}\right)^2 \frac{(1-2x)^2}{x} & \text{bosonic decay,} \\ \frac{y_\psi^2}{64\pi^3} \left(\frac{m_\phi}{M_P}\right)^2 \frac{(1-2x)}{x} [2x(x-1)+1] & \text{fermionic decay,} \end{cases} \quad (4)$$

where  $x \equiv E_\omega/m_\phi$  and with a graviton energy spanning the range

$$0 < E_\omega \leq m_\phi/2 \quad \text{or} \quad 0 < x \leq 1/2. \quad (5)$$

We note that a graviton can carry a maximum of half of the inflaton energy, which occurs when the daughter particle mass approaches zero. In such case, the differential decay rate tends toward zero as the phase space closes. This is why the differential decay rate goes to zero when  $x \rightarrow 1/2$ . Moreover, we note that when  $x \rightarrow 0$ , the spectrum  $\frac{d\Gamma^{1\rightarrow 3}}{dE_\omega} \rightarrow \infty$ , which is a well-known feature of (infrared) graviton Bremsstrahlung [8]. In this work, our main interest lies in quantities proportional to  $\frac{d\Gamma^{1\rightarrow 3}}{dE_\omega} E_\omega$ , so we do not need to worry about the divergence here. However, to address such divergence, it is necessary to include vertex and self-energy diagrams<sup>1</sup> [9].

### 3. Gravitational Wave Spectrum

After being produced from inflaton decays, gravitons propagate throughout the universe, giving rise to a homogeneous and isotropic stochastic gravitational wave (GW) background. The GW spectrum  $\Omega_{\text{GW}}(f)$  at present, defined for a frequency  $f$ , is characterized by:

$$\Omega_{\text{GW}}(f) \equiv \frac{1}{\rho_c} \frac{d\rho_{\text{GW}}}{d\ln f} = \Omega_\gamma^0 \frac{g_\star(T_{\text{rh}})}{g_\star(T_0)} \left[ \frac{g_{\star s}(T_0)}{g_{\star s}(T_{\text{rh}})} \right]^{4/3} \frac{d(\rho_{\text{GW}}(T_{\text{rh}})/\rho_R(T_{\text{rh}}))}{d\ln E_\omega}. \quad (6)$$

<sup>1</sup>This is similar to the situation in QED.

Here,  $g_\star(T)$  and  $g_{\star s}(T)$  represent the numbers of relativistic degrees of freedom contributing to the total radiation and entropy, respectively. The quantity  $\rho_c$  represents the critical energy density, and  $\Omega_\gamma^0 h^2 \simeq 2.47 \times 10^{-5}$  denotes the observed photon abundance at present. The graviton energy  $E_\omega$  in Eq. (6) is related to the frequency  $f$  as follows<sup>2</sup>:

$$E_\omega = 2\pi f \frac{a_0}{a_{\text{rh}}} = 2\pi f \frac{T_{\text{rh}}}{T_0} \left[ \frac{g_{\star s}(T_{\text{rh}})}{g_{\star s}(T_0)} \right]^{1/3}, \quad (7)$$

which accounts for the redshift of the graviton energy from the end of reheating to the current epoch. In the last step, we have utilized the assumption that entropy is conserved after reheating, allowing us to rewrite  $a_0/a_{\text{rh}}$ .

The differential GW energy spectrum at the end of reheating takes a form [5]

$$\frac{d(\rho_{\text{GW}}(T_{\text{rh}})/\rho_{\text{R}}(T_{\text{rh}}))}{dE_\omega} \simeq \left( \frac{d\Gamma^{1 \rightarrow 3}}{dE_\omega} \frac{1}{\Gamma^{1 \rightarrow 2}} \right) \left( \frac{E_\omega}{m_\phi} \right) \left[ 1 - \left( \frac{T_{\text{rh}}}{T_{\text{max}}} \right)^{8/3} \right], \quad (8)$$

where  $T_{\text{max}}$  denotes that maximum of the temperature during reheating. In Eq. (8), the first part denotes the differential branching ratio for the inflaton decaying into gravitons, the second piece corresponds to the fraction of energy transferred to gravitons in each decay, and the last term arises from the entropy dilution during reheating. It's worth mentioning that under the assumption of instantaneous decay of the inflaton, the expression within the square brackets simplifies to unity. Using  $\Gamma^{1 \rightarrow 2}$  and  $\frac{d\Gamma^{1 \rightarrow 3}}{dE_\omega}$  from Section 2, we obtain [5]:

$$\Omega_{\text{GW}}(f) \simeq C_{\Omega_{\text{GW}}} \left( \frac{T_{\text{rh}}}{5.5 \times 10^{15} \text{ GeV}} \right) \left( \frac{m_\phi}{M_{\text{P}}} \right) \left( \frac{f}{10^{12} \text{ Hz}} \right), \quad (9)$$

where  $C_{\Omega_{\text{GW}}}$  takes values of approximately  $1.4 \times 10^{-8}$  for scalars and  $2.8 \times 10^{-8}$  for fermions.

Note that the differential graviton production rate takes the form  $\frac{d\Gamma^{1 \rightarrow 3}}{dE_\omega} \propto \frac{1}{E_\omega}$  (cf. Eq. (4)). Consequently, the GW spectrum  $\Omega_{\text{GW}} \propto E_\omega$ , explaining why the spectrum is linearized in  $f$ . Since the maximum graviton energy is  $m_\phi/2$ , it is important to note that Eq. (9) applies for frequencies  $f$  satisfying

$$f \lesssim \frac{m_\phi}{4\pi} \frac{T_0}{T_{\text{rh}}} \left[ \frac{g_{\star s}(T_0)}{g_{\star s}(T_{\text{rh}})} \right]^{1/3} \simeq 4.1 \times 10^{12} \left( \frac{m_\phi}{M_{\text{P}}} \right) \left( \frac{5.5 \times 10^{15} \text{ GeV}}{T_{\text{rh}}} \right) \text{ Hz}, \quad (10)$$

where  $T_0 = 2.73 \text{ K}$ ,  $g_{\star s}(T_0) = 3.94$  and  $g_{\star s}(T_{\text{rh}}) = 106.75$  have been utilized. We can further calculate the dimensionless strain parameter, defined as [13]:

$$h_c(f) = \frac{1}{f} \sqrt{\frac{3 H_0^2 \Omega_{\text{GW}}(f)}{2\pi^2}} = 1.26 \times 10^{-18} \left( \frac{\text{Hz}}{f} \right) \sqrt{h^2 \Omega_{\text{GW}}(f)}, \quad (11)$$

where  $H_0 \equiv H(T_0) \simeq 1.44 \times 10^{-42} \text{ GeV}$  corresponds to the Hubble parameter at present.

In Fig. 2, we present the dimensionless strain  $h_c$  as a function of the gravitational wave frequency  $f$ . Furthermore, the figure includes sensitivity curves from several proposed GW

<sup>2</sup>Here, we use the Planck-Einstein relation between energy and frequency:  $E = 2\pi\hbar f$ . In high energy physics, natural units with  $\hbar = 1$  are commonly employed.

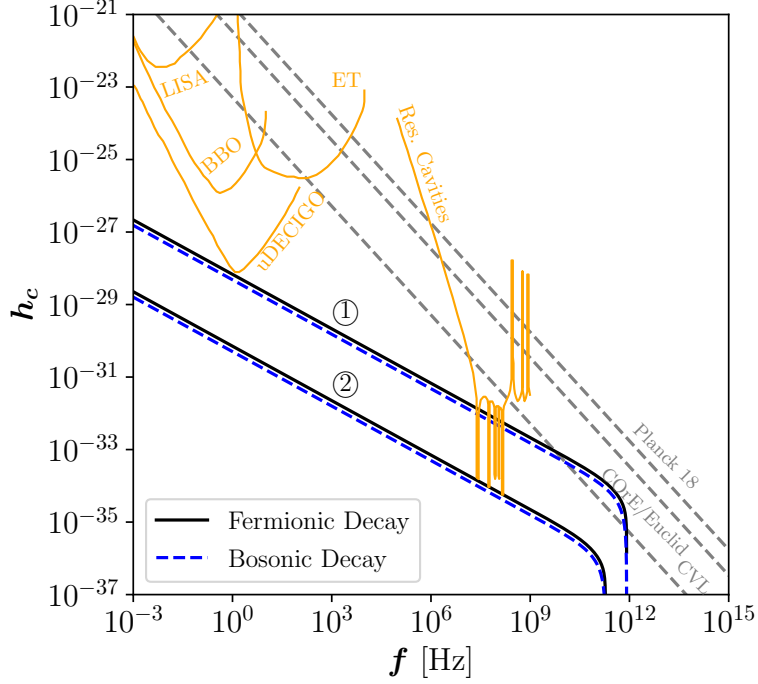


**Figure 2:** The dimensionless strain  $h_c$  as a function of the gravitational wave frequency  $f$ , considering two benchmarks ① and ② outlined in the main text. The black solid and blue dashed dotted curves represent decays into fermionic and bosonic final states with an additional graviton, respectively.

detectors, encompassing LISA [14], the Einstein Telescope (ET) [15], the Big Bang Observer (BBO) [16], ultimate DECIGO (uDECIGO) [17], and resonant cavities [18]. These sensitivity curves have been adapted from Refs. [19, 20]. We refer to [21] for a review on high frequency GW searches. Note that the energy stored in GWs shares characteristics akin to those of dark radiation, thereby contributing to the effective number of neutrino species denoted as  $N_{\text{eff}}$ . Here, we present a compilation of various constraints related to this. The Planck 2018 established a result at 95% confidence level:  $N_{\text{eff}} = 2.99 \pm 0.34$ . Future experiments, such as COrE and Euclid, are expected to further improve these constraints at the  $2\sigma$  level, yielding  $\Delta N_{\text{eff}} \lesssim 0.013$ . It is also interesting to mention a bound  $\Delta N_{\text{eff}} \lesssim 3 \times 10^{-6}$  based on a hypothetical cosmic-variance-limited (CVL) CMB polarization experiment [22].

We have considered two sets of model parameters: ①  $m_\phi = M_P/5$  and  $T_{\text{rh}} = 5.5 \times 10^{15}$  GeV, and ②  $m_\phi = M_P/10^3$  and  $T_{\text{rh}} = M_P/(2 \times 10^4)$ . For larger  $m_\phi$  and  $T_{\text{rh}}$ , the signal is larger as implied in Eq. (9). The curves bend when the frequency  $f$  reaches to upper limit shown in Eq. (10). We note that for large inflaton masses, resonant cavity detectors could potentially probe the signal at the high-frequency regime, while detectors like uDECIGO might catch the lower frequency part of the spectrum. However, constructing a viable inflation model with these parameters while satisfying current CMB constraints may not be straightforward.

#### 4. Probing Reheating with Graviton Bremsstrahlung

So far, we have assumed that the inflaton oscillates in a quadratic potential  $\sim \phi^2$ . In this section, we generalize our discussion to a general potential  $\sim \phi^n$  with  $n > 2$ , which can be realized, for example, in the attractor inflation models [10]. As mentioned earlier, the effect of entropy dilution during reheating also manifests in the GW spectrum (cf. Eq. (8)).

In the case of a quadratic potential with  $n = 2$ , the reheating dynamics are similar for both bosonic and fermionic decay. Consequently, the dilution effect on the GW spectrum is similar. However, for  $n > 2$ , the difference becomes prominent. For bosonic reheating, the inflaton decay rate  $\Gamma_b^{1 \rightarrow 2} \propto 1/m_\phi$  (cf. Eq. (2)), while for fermionic reheating  $\Gamma_f^{1 \rightarrow 2} \propto m_\phi$  (cf. Eq. (2)). Note that for  $n > 2$ , the inflaton mass is not constant and takes the form  $m_\phi \propto \phi^{n-2}$  with  $\phi$  being a decaying function with time [11, 12], resulting in the radiation released in the bosonic reheating case tends to be suppressed. Consequently, the GW spectrum in the bosonic reheating scenario can be boosted. This provides an intuitive picture, and we refer interested readers to [6] for more computational details.

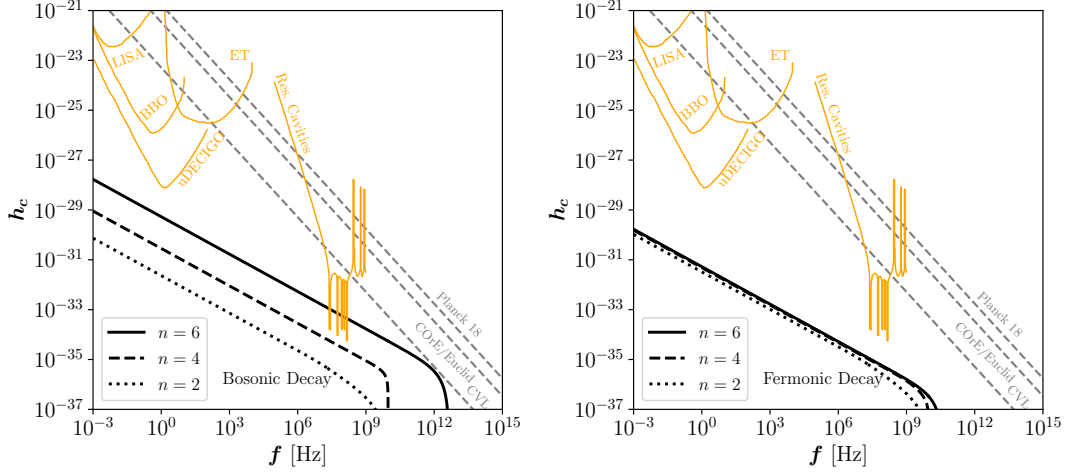


**Figure 3:** The dimensionless strain  $h_c$  as a function of the gravitational wave frequency  $f$  and  $n$ . The left frame and right frame correspond to the spectrum for inflaton bosonic and fermionic decay, respectively.

In Fig. 3, we present the spectrum by varying the value of  $n$  with much smaller model parameters:  $m_\phi(T_{\text{rh}}) \simeq 10^{13}$  GeV,  $T_{\text{rh}} \simeq m_\phi(T_{\text{rh}})$  and  $T_{\text{max}}/T_{\text{rh}} = 10$ . As argued earlier, we see that the spectrum can be boosted in the bosonic case, whereas the enhancement in the fermionic reheating scenario is not as prominent. This is particularly interesting because future high-frequency GW detectors, such as the resonant cavity detector, could be used to probe the dynamics of reheating. If a null result is obtained, we could potentially rule out certain regions of the model parameter space in the bosonic reheating scenario.

#### 5. Conclusions

To summarize, in this talk, I show that inflaton decay is an inevitable and interesting source of gravitational waves (GW) via graviton Bremsstrahlung during inflationary reheating. For an inflaton

oscillating in a quadratic potential  $\sim \phi^2$ , the GW spectrum is linear with respect to frequency  $f$  and exhibits a peak in the ultra-high-frequency regime, as depicted in Fig. 2. In such cases, a large inflaton mass and reheating temperature are necessary to produce a sizable signal. When the inflaton oscillates in a potential  $\sim \phi^n$ , with  $n > 2$ , we observe that the signal can be amplified in a bosonic reheating scenario due to the suppression of entropy dilution. The enhancement on the GW spectrum increases with  $n$ , as demonstrated in Fig. 3. By highlighting the distinct features in the GW spectrum, we emphasize that graviton Bremsstrahlung offers a novel pathway for probing the dynamics of reheating, including the type of inflaton-matter coupling and the shape of the inflaton potential.

## Acknowledgments

This article is based on the talk given at the “Workshop on Theoretical Particle Cosmology in the Early and Late Universe”, organized by EUROPEAN INSTITUTE FOR SCIENCES AND THEIR APPLICATIONS (EISA) and Mainz Institute for Theoretical Physics (MITP) in Corfu, Greece. I am grateful to the organizers for providing me with the opportunity to present in such a beautiful location. The original works [5, 6] were done in collaboration with B. Barman, N. Bernal and O. Zapata. I acknowledge the support from the Cluster of Excellence “Precision Physics, Fundamental Interactions, and Structure of Matter” (PRISMA+ EXC 2118/1) funded by the Deutsche Forschungsgemeinschaft (DFG, German Research Foundation) within the German Excellence Strategy (Project No. 390831469).

## References

- [1] D. H. Lyth and A. R. Liddle, “The primordial density perturbation: Cosmology, inflation and the origin of structure.”
- [2] L. Kofman, A. D. Linde and A. A. Starobinsky, *Phys. Rev. D* **56** (1997), 3258-3295 doi:10.1103/PhysRevD.56.3258 [arXiv:hep-ph/9704452 [hep-ph]].
- [3] K. Nakayama and Y. Tang, *Phys. Lett. B* **788** (2019), 341-346 doi:10.1016/j.physletb.2018.11.023 [arXiv:1810.04975 [hep-ph]].
- [4] D. Huang and L. Yin, *Phys. Rev. D* **100** (2019) no.4, 043538 doi:10.1103/PhysRevD.100.043538 [arXiv:1905.08510 [hep-ph]].
- [5] B. Barman, N. Bernal, Y. Xu and Ó. Zapata, *JCAP* **05** (2023), 019 doi:10.1088/1475-7516/2023/05/019 [arXiv:2301.11345 [hep-ph]].
- [6] B. Barman, N. Bernal, Y. Xu and Ó. Zapata, *Phys. Rev. D* **108** (2023) no.8, 083524 doi:10.1103/PhysRevD.108.083524 [arXiv:2305.16388 [hep-ph]].
- [7] S. Y. Choi, J. S. Shim and H. S. Song, *Phys. Rev. D* **51** (1995), 2751-2769 doi:10.1103/PhysRevD.51.2751 [arXiv:hep-th/9411092 [hep-th]].
- [8] S. Weinberg, *Phys. Rev.* **140** (1965), B516-B524 doi:10.1103/PhysRev.140.B516

- [9] B. M. Barker, S. N. Gupta and J. Kaskas, *Phys. Rev.* **182** (1969), 1391-1396 doi:10.1103/PhysRev.182.1391
- [10] R. Kallosh and A. Linde, *JCAP* **07** (2013), 002 doi:10.1088/1475-7516/2013/07/002 [arXiv:1306.5220 [hep-th]].
- [11] M. A. G. Garcia, K. Kaneta, Y. Mambrini and K. A. Olive, *JCAP* **04** (2021), 012 doi:10.1088/1475-7516/2021/04/012 [arXiv:2012.10756 [hep-ph]].
- [12] N. Bernal and Y. Xu, *JCAP* **12** (2022), 017 doi:10.1088/1475-7516/2022/12/017 [arXiv:2209.07546 [hep-ph]].
- [13] M. Maggiore, *Phys. Rept.* **331** (2000), 283-367 doi:10.1016/S0370-1573(99)00102-7 [arXiv:gr-qc/9909001 [gr-qc]].
- [14] P. Amaro-Seoane *et al.* [LISA], [arXiv:1702.00786 [astro-ph.IM]].
- [15] M. Maggiore, C. Van Den Broeck, N. Bartolo, E. Belgacem, D. Bertacca, M. A. Bizouard, M. Branchesi, S. Clesse, S. Foffa and J. García-Bellido, *et al.* *JCAP* **03** (2020), 050 doi:10.1088/1475-7516/2020/03/050 [arXiv:1912.02622 [astro-ph.CO]].
- [16] G. M. Harry, P. Fritschel, D. A. Shaddock, W. Folkner and E. S. Phinney, *Class. Quant. Grav.* **23** (2006), 4887-4894 [erratum: *Class. Quant. Grav.* **23** (2006), 7361] doi:10.1088/0264-9381/23/15/008
- [17] H. Kudoh, A. Taruya, T. Hiramatsu and Y. Himemoto, *Phys. Rev. D* **73** (2006), 064006 doi:10.1103/PhysRevD.73.064006 [arXiv:gr-qc/0511145 [gr-qc]].
- [18] N. Herman, L. Lehoucq and A. Fúzfá, *Phys. Rev. D* **108** (2023) no.12, 124009 doi:10.1103/PhysRevD.108.124009 [arXiv:2203.15668 [gr-qc]].
- [19] A. Ringwald, J. Schütte-Engel and C. Tamarit, *JCAP* **03** (2021), 054 doi:10.1088/1475-7516/2021/03/054 [arXiv:2011.04731 [hep-ph]].
- [20] A. Ringwald and C. Tamarit, *Phys. Rev. D* **106** (2022) no.6, 063027 doi:10.1103/PhysRevD.106.063027 [arXiv:2203.00621 [hep-ph]].
- [21] N. Aggarwal, O. D. Aguiar, A. Bauswein, G. Cella, S. Clesse, A. M. Cruise, V. Domcke, D. G. Figueroa, A. Geraci and M. Goryachev, *et al.* *Living Rev. Rel.* **24** (2021) no.1, 4 doi:10.1007/s41114-021-00032-5 [arXiv:2011.12414 [gr-qc]].
- [22] I. Ben-Dayan, B. Keating, D. Leon and I. Wolfson, *JCAP* **06** (2019), 007 doi:10.1088/1475-7516/2019/06/007 [arXiv:1903.11843 [astro-ph.CO]].